

DECREASE IN GROUND-RUN DISTANCE OF AIRPLANES BY APPLYING ELECTRICALLY DRIVEN WHEELS

Hiroshi Kobayashi*, Akira Nishizawa*
*Japan Aerospace Exploration Agency

Keywords: *STOL, electric motor, driving wheel*

Abstract

A new takeoff method for small airplanes that employs electrically driven landing gear is proposed. Experiments using a model airplane driven by electrically powered wheels showed that the ground-run distance is decreased by half by using a combination of powered wheels and propeller without an increase of energy consumption during the ground-roll. A study was also conducted of the trade-off between the ground-run distance and flight performance of a full-size propeller airplane assuming that the motors and controllers of an existing electric vehicle were used to power the landing gear.

1 Introduction

To improve the convenience of air transportation systems, Short Take-Off and Landing (STOL) is a beneficial characteristic for any size of airplane. Applying powered high-lift systems is an effective method for achieving this goal[1],[2],[3]. However, such systems usually require airplane wings to be equipped with specially designed aerodynamic powered devices to achieve sufficient lift.

We propose a new method to decrease ground-run distance using landing gear driven by electric motors to augment the thrust of the engines. This system can be easily added to existing airplanes without changing aerodynamic designs.

In comparison with internal combustion engines, electric motors are generally very efficient and operate without producing exhaust gas or intense noise. Although past electric motor systems had the disadvantage of a small power-to-weight ratio, recent improvement of

permanent magnet characteristics and breakthroughs in battery technology enable us to apply light and powerful electric motor systems[4] to airplanes.

The idea of using electrically driven landing gear to cut fuel consumption and decrease noise during taxiing is not new. Methods to drive landing gear by electric motors were demonstrated in the 1970s[5] and have been studied in recent years[6],[7],[8]. The present study is different from these because it considers not only taxiing but also ground-run.

In this study, the effectiveness of an electrically driven wheels system (EDWS) is demonstrated experimentally using a scale model. Also, the equations predicting ground-run distance when employing an EDWS are derived; these reveal the relationship between ground-run distance and the design parameters of an EDWS. Furthermore the feasibility of an EDWS is discussed on the assumption that existing electric motor systems are applied to a small propeller airplane for general aviation.

2 Experimental Setup and Conditions

2.1 Model

Figure 1 shows a 19% scale model of Cessna Skylane 182, which was used for the preliminary wind tunnel tests and the ground-run tests. The EDWS of the model was installed to the rear wheels because the normal force acting on the front wheel is so small that not enough thrust is obtained if the front wheel is driven.

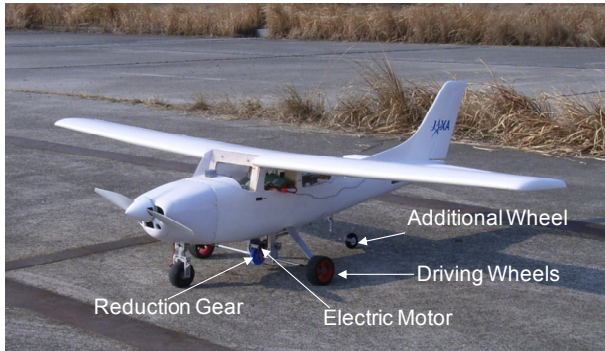


Fig. 1 19% scale model for the ground-run test.

When an EDWS is used in ground roll, a large pitch-up moment acts on the model because the thrust of the EDWS acts on a point below the center of gravity. Therefore, the rear-wheel drive has the disadvantage that the pitch-up motion causes the tail to contact with runway. To prevent such unfavorable motion an additional wheel was installed aft of the center of gravity.

The EDWS of the model is removable to enable the comparison of ground-run distances between different configurations (with or without the EDWS). Table 1 shows the specifications of the model in each configuration.

Table 1 Specifications of the scale model

Model configuration	Without EDWS	With EDWS
Length	1.64m	
Span	2.06m	
Wing area S	0.587m ²	
C_L	0.58	
C_D	0.048	
Mass m	6.77kg	7.85kg
T_p/mg	0.33	0.29
V_{TO}	13.0m/s	14.0m/s
Electric motor for EDWS	ModelMotors AXI2826/12($K_v=760$ [rpm/V], 0.181kg)	
Battery for EDWS	Li-Po 5s (18.5V in nominal terms)	
Wheel	Dia : $2r=88$ mm Width:40mm	
Gear ratio G	3.3	
Propeller	Dia:18inch, Pitch:12inch	
Electric motor for propeller	ModelMotors AXI5330/24 (0.652kg)	
Battery for propeller	Li-Po 7s (25.9V in nominal terms)	

Takeoff velocity V_{TO} is defined by multiplying the stall speed of the model by 1.2 in this study. The stall speed of the model is calculated using the maximum lift coefficient $C_{Lmax} = 1.59$ found from preliminary wind tunnel tests[9]. Without the EDWS, the mass of the model is $m = 6.77$ kg and $V_{TO} = 13.0$ m/s. On the other hand, with the EDWS, $m = 7.85$ kg and V_{TO} increases to 14.0m/s.

The propeller and wheels of the model are independently driven by brushless motors powered by lithium-polymer batteries. Each motor's output is controlled by a motor controller receiving pulse-width modulated signals from a radio control transmitter and receiver set.

In the model, some sensors are installed to monitor the condition of the model and energy consumption. Outputs from the sensors are sampled at 100Hz and logged by a 12-bit data logger mounted on the model.

2.2 Experimental Conditions

The ground-run tests were conducted on a dry asphalt runway with three ground-run methods. Descriptions of these methods, labeled (a), (b) and (c), are given in Table 2.

Table 2 Ground-run methods

Method	(a)	(b)	(c)
Model configuration	Without EDWS	With EDWS	
Propeller thrust	Applied	None	Applied
Wheel thrust	None	Applied	Applied
Starting procedure	1) Hold the model and raise the propeller revolution to maximum. 2) Release the model.	1) Rapidly increase the EDWS power from zero to maximum.	1) Hold the model and raise the propeller revolution to maximum. 2) Release the model 3) Rapidly increase the EDWS power from zero to maximum

For each method, the velocity was increased from zero to V_{TO} during one run. Ground-run distance L_0 is defined as the distance from the starting position to the position where the velocity reaches V_{TO} . Each L_0 is normalized by the value of L_0 for method (a), L_{0a} .

3 Analytical Methods and Validation

3.1 Model for Friction between Runway and Tires

The thrust of the EDWS, T_w , is generated by friction between the runway and tires. Thus, the maximum value of T_w is given by

$$T_{wmax} = W\mu \quad (1),$$

where μ is the coefficient of static friction between the runway and tires and W is the normal force acting on the runway. It is known that μ is a function of the slip ratio

$$\lambda = \frac{r\omega - V}{r\omega} \quad (2),$$

where r is radius of the wheels and ω is the rotational speed of the tires. Based on the mathematical model proposed by Pacejka et al.[10], $\mu(\lambda)$ is assumed to be

$$\mu = \mu_{max} \sin[1.65 \arctan\{\beta\lambda - \varepsilon(\beta\lambda - \arctan \beta\lambda)\}] \quad (3),$$

where μ_{max} , β and ε are constants determined by runway condition and the materials and shape of the tires. Preliminary ground-run tests[9] determined these constants to be $\mu_{max} = 0.53$, $\beta = 6$, and $\varepsilon = 0.56$. Figure 2 shows $\mu(\lambda)$ as predicted by equation (3) and measured in the preliminary tests.

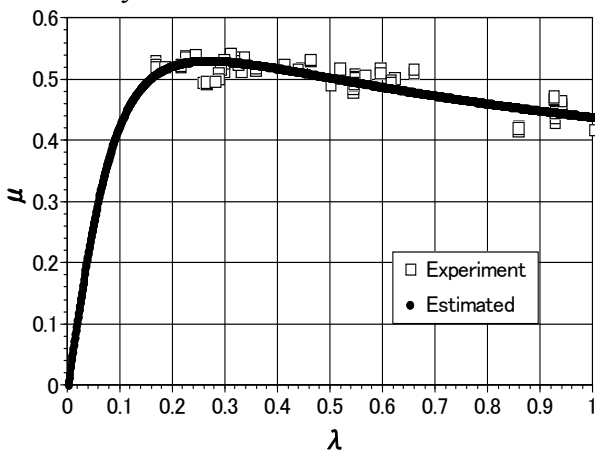


Fig. 2 Variation of the coefficient of static friction, μ , between dry asphalt and the tires of the scale model with the slip ratio, λ .

3.2 Torque Characteristics of DC Brushless Motors

In this study, a DC brushless motor is used as the power-train of the EDWS. When the output of the motor is at a maximum, the voltage of the power supply E can be described by

$$E = \frac{N_m}{K_v} + IR \quad (4),$$

where N_m is the rotational speed of the motor, K_v is the back electromotive force coefficient, R is the electrical resistance of the circuit including the motor and I is the current in the circuit. Also, using the zero-torque current I_0 , the torque of the motor τ can be described by

$$\tau = \frac{(I - I_0)}{K_v} \quad (5).$$

When the motor outputs maximum torque τ_{max} , eliminating I from equations (4) and (5) we have

$$E = \frac{N_m}{K_v} + R(K_v\tau_{max} + I_0) \quad (6).$$

Furthermore, because N_m is the product of ω and the gear ratio between the motor and tires G ,

$$E = \frac{G\omega}{K_v} + R(K_v\tau_{max} + I_0) \quad (7),$$

where RI_0 is usually negligibly small compared to the other terms.

On the other hand, the relationship of T_w and τ is given by

$$T_w = \frac{G\tau}{r} \quad (8).$$

Thus, using equations (7) and (8), T_{wmax} can also be written as

$$T_{wmax} = \left(\frac{G}{K_v}\right) \left\{ E - \left(\frac{G}{K_v}\right)\omega \right\} \frac{1}{Rr} \quad (9).$$

3.3 Transition of T_{wmax}

To minimize L_0 , T_w must be maximized consistently. As previously mentioned, T_w is limited to the values described in equations (1)

and (9). Thus, $T_{w \max}$ is equal to the smaller of the two values given by equations (1) and (9).

When λ is controlled to be the constant λ_{\max} which maximizes μ , we see from equation (2) that ω is proportional to V :

$$\omega = \frac{V}{r(1 - \lambda_{\max})} = c_4 V \quad (10).$$

Using equations (9) and (10), equations relating $T_{w \max}$ and V can be written:

$$T_{w \max} = \begin{cases} W\mu_{\max} & (W\mu_{\max} \leq -c_2\omega + c_3) \\ -c_2c_4V + c_3 & (W\mu_{\max} > -c_2\omega + c_3) \end{cases} \quad (11),$$

where setting c_2 and c_3 equal to $T_{w \max}$ in equation (11) gives the theoretical maximum value for a specified μ_{\max} . To maintain λ equal to a specified value, current control methods[11] used for electric vehicles (EVs) are expected to be effective.

3.4 Equation of Motion

When T_w is maximized, the equation of motion for the airplane equipped with the EDWS is

$$m \left(\frac{dV}{dt} \right) = T_p + T_{w \max} - D_a - D_r \quad (12),$$

where T_p is thrust of the propeller, D_a is the aerodynamic drag and D_r is the rolling resistance between the runway and tires. From preliminary wind tunnel tests, the thrust coefficient $C_T = T_p / (\rho N_p^2 D_p^4)$ of the propeller used for the scale model can be assumed to be

$$C_T = -C_0 (V / N_p D_p)^2 + C_1 \quad (13).$$

Then, W , D_a and D_r are described by

$$W = mg - \frac{1}{2} \rho V^2 S C_L \quad (14)$$

$$D_a = \frac{1}{2} \rho V^2 S C_D \quad (15)$$

$$D_r = (mg - \frac{1}{2} \rho V^2 S C_L) \mu_{\text{roll}} \quad (16),$$

where N_p , D_p , ρ , S and μ_{roll} are the rotational speed of the propeller, the diameter of the

propeller, air density, the wing area of the model and the coefficient of rolling friction, respectively. Using equations (13) – (16), an ordinary differential equation can be derived from equation (12) as follows.

$$m \left(\frac{dV}{dt} \right) = \begin{cases} -(C_0 + C_\mu)V^2 + C_2 + mg\mu_{\max} & (W\mu_{\max} \leq -c_2\omega + c_3) \\ -C_0V^2 - C_1V + C_2 + C_3 & (W\mu_{\max} > -c_2\omega + c_3) \end{cases} \quad (17).$$

$$(C_\mu = \frac{1}{2} \rho S C_L \mu_{\max}, C_0 = c_0 \rho D_p^2 + \frac{1}{2} \rho S C_D - \frac{1}{2} \rho S C_L \mu_{\text{roll}},$$

$$C_1 = c_2 c_4, C_2 = c_1 \rho N_p^2 D_p^4 - mg \mu_{\text{roll}}, C_3 = c_3)$$

From this equation, general analytical solutions can be obtained:

$$V(t) = \begin{cases} A_1 \coth(C_{a0}t + C_{a1}) & (W\mu_{\max} \leq -c_2\omega + c_3) \\ B_1 \coth(C_{b0}t + C_{b1}) + B_3 & (W\mu_{\max} > -c_2\omega + c_3) \end{cases} \quad (18),$$

where C_{a1} and C_{b1} are arbitrary constants of an initial-value problem.

$$A_1 = \left(\frac{C_2 + mg\mu_{\max}}{C_0 + C_\mu} \right)^{\frac{1}{2}}, \quad C_{a0} = \frac{A_1(C_0 + C_\mu)}{m},$$

$$B_1 = \left\{ \frac{C_2 + C_3}{C_0} + \left(\frac{C_1}{2C_0} \right)^2 \right\}^{\frac{1}{2}}, \quad C_{b0} = \frac{B_1 C_0}{m},$$

$$B_3 = \frac{C_1}{2C_0}.$$

Thus, by integrating equation (18), the distance from the start position of the ground-run $L(t)$ can be described by

$$L(t) = \begin{cases} A_2 \ln\{\sinh(C_{a0}t + C_{a1})\} + C_{a2} & (W\mu_{\max} \leq -c_2\omega + c_3) \\ B_2 \ln\{\sinh(C_{b0}t + C_{b1})\} + B_3 t + C_{b2} & (W\mu_{\max} > -c_2\omega + c_3) \end{cases} \quad (19),$$

$$(A_2 = \frac{A_1}{C_{a0}}, \quad B_2 = \frac{B_1}{C_{b0}})$$

where C_{a2} and C_{b2} are also arbitrary constants of an initial-value problem. The distance $L(t)$ predicted using equation (19) is the theoretical minimum value because $T_{w \max}$ in equation (11) is the theoretical maximum value.

3.5 Validation

The values of $L(t)/L_{0a}$ for methods (a) and (c) predicted using equation (19) are compared to the measured values in Fig. 3. The differences between the predicted and measured values are less than about 7% of the measured L_{0a} , indicating the validity of the prediction method.

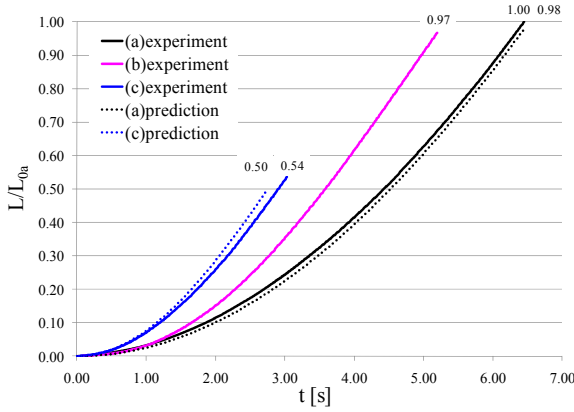


Fig. 3 Comparison between predicted and experimental ground-run distances for three ground-run methods.

4 Results

4.1 Ground-run Distance

Figure 3 shows the ground-run distance $L(t)/L_{0a}$ obtained by the three methods. By applying method (c), which couples the thrusts of the propeller and the EDWS, L_0/L_{0a} is decreased by one half compared to that of method (a) which uses only the propeller thrust. The results show the effectiveness of the ground-run method proposed in this study.

Figure 4 shows the relation between V/V_{TO} and acceleration a (normalized by the acceleration due to gravity g) during the ground-run. It is found that the accelerations using the EDWS (methods (b) and (c)) are much higher than that without the EDWS (method (a)).

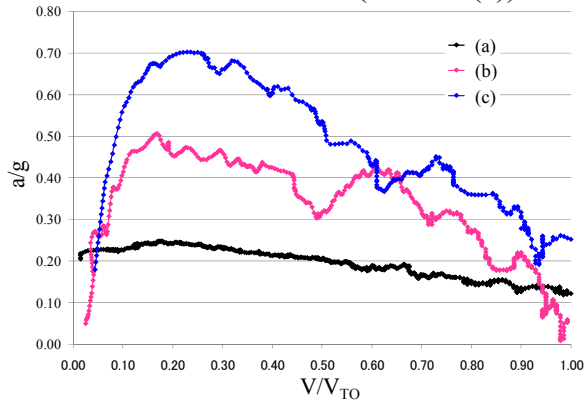


Fig. 4 Acceleration vs. velocity for each ground-run method.

Although a/g for method (b) is almost twice that of method (a) at $V/V_{TO} < 0.5$, the ground-run distances are not so different (see Fig. 3). The reason why method (b) cannot decrease L_0/L_{0a}

drastically is that it takes considerable time to accelerate the model when V/V_{TO} exceeds 0.95.

4.2 Efficiency

Figure 5 shows propulsion efficiency

$$\eta_p = \frac{TV}{EI} \quad (20).$$

As shown in Fig. 5, the value of η_p for method (b) is the highest at almost all V/V_{TO} and this feature of η_p becomes more prominent when V/V_{TO} is large. This fact indicates that EDWS has an advantage in terms of energy consumption not only for taxiing but also for ground-run.

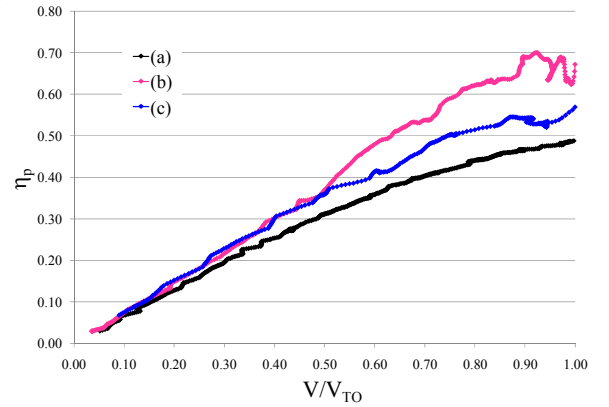


Fig. 5 Propulsion efficiency vs. velocity for each ground-run method.

4.3 Design Parameters

When designing an EDWS, various factors should be taken into consideration, including the selection of electric motors and batteries, and the structure of the landing gear including drive system. As described in equations (1), (9) and (14), when r , C_L , and μ_{max} are known, the relationship between V and T_{wmax} is governed by E , G/K_v and R ; here, R is the sum of electrical resistances of the motor coils, power lines and the motor controller. To simplify the following discussion, R is assumed to be constant. Thus, in the conceptual design phase, a combination of K_v , G and E for achieving the required L_0 must be determined.

Figure 6 shows L_0/L_{0a} for method (c) with various values of G/K_v and numbers of battery cells (1 cell: 3.7V) in series. As shown in Fig. 6, L_0/L_{0a} becomes smaller for higher E . This is because, for high E , T_{wmax} can be kept large for

large ω or large V as described in equations (9) and (10).

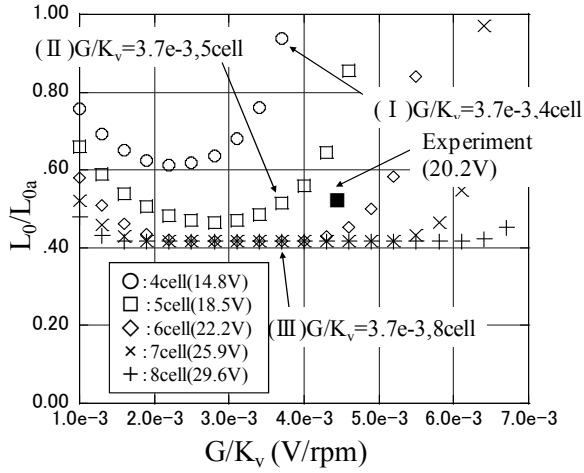


Fig. 6 Analytical and experimental results of the relation between L_0/L_{0a} and G/K_v for various numbers of Li-Po battery cells in series for the scale model.

An optimum value of G/K_v exists which minimizes L_0/L_{0a} for each number of cells. On the other hand, for more than 6 cells in series, L_0/L_{0a} is limited to a certain value independent of G/K_v and E . This is when $W\mu_{\max}$ is consistently less than $-c_2\omega + c_3$ as described in equation (17). Therefore, L_0/L_{0a} cannot be decreased by increasing the number of battery cells in such cases because $T_{w\max}$ is limited by only friction between the runway and tires.

5 Conceptual Design for Small Airplanes

In this section, the application of an EDWS to a Cessna Skyhawk 172 is discussed. Table 3 shows the specifications of the Cessna Skyhawk 172[12],[13].

Table 3 Specifications of Cessna Skyhawk 172

Number of seats	4
Maximum take-off weight	10900N
Empty weight	7122N
Wing area	16.2m ² (174ft ²)
Stall velocity	Flaps NOT deployed: 26.1m/s Flaps deployed (30°): 24.2m/s
Diameter of propeller	1.905m (75in.)
Propeller revolution	40Hz (2400rpm)
Engine output	120kW (160HP)
Diameter of tires	0.44m (17.5in.)
Ground-run distance L_{0a}	288m

The maximum lift coefficients $C_{L\max}$ are estimated as 1.6 and 2.1 from the stall speeds at flap angles of $\delta_f = 0$ and 30° , respectively.

Assuming that $C_{L\max}$ is proportional to δ_f , $C_{L\max}$ is 1.93 at takeoff ($\delta_f = 20^\circ$) and the stall speed is 24.0m/s. Then, $V_{TO} = 1.2 \times 24.0 = 28.8$ m/s. To simplify the following discussion, the aerodynamic coefficients and friction characteristics during ground-run are assumed to be $C_D = C_{D\min} = 0.0341$, $C_L = 0.0$, $\lambda_{\mu\max} = 0.1$ and $\mu_{\max} = 1.05$. The friction coefficient assumed above is equivalent to that between ordinary bias tires and dry asphalt[14].

Considering recent improvements in performance, the motor systems used for EVs are supposed to be suitable for use in an EDWS. Table 4 shows the specifications of electric motor systems of typical EVs.

Table 4 Specifications of motor systems for EV

Model	KAZ	ALTRA-EV	EV PLUS
Maker	Keio University	Nissan	Honda
K_v	0.73Hz/V	1.21Hz/V	0.16Hz/V
P_{\max}	55kW	62kW	49kW
T_{\max}	100Nm	175Nm	275Nm
$N_{P\max}$	150Hz	267Hz	28.3Hz
E_{\max}	315V	336V	288V
W_m	216N	368N	441N
W_c	490.5N (for 2 wheels)	147N	

Generally, when size of the motor becomes large, the resistance of the motor coils R_c tends to be large, becoming the dominant contribution to R . Thus, R is assumed to be equal to R_c and the resistance of the motor used for KAZ (0.5ohm) is adopted as R_c in this section. Then, K_v of the motor can be obtained from equation (4) as

$$K_v = \frac{N_{P\max}}{E_{\max} - IR} \quad (21),$$

where $N_{P\max}$ is the rotational speed of the motor at maximum output and E_{\max} is the maximum voltage of the motor controller. Also, I is estimated using the efficiency of the motor system η_m :

$$I = \frac{P_{\max} R}{E_{\max} \eta_m} \quad (22),$$

where P_{\max} is the maximum output of the motor and η_m is assumed to be 0.8.

Figure 7 shows the relationship between L_0/L_{0a} and G/K_v for a Cessna Skyhawk 172 equipped with an EDWS. In addition, a nominal ground-run distance of 288m is used as L_{0a} . As shown in Fig. 7, L_0/L_{0a} decreased to 0.41 at $G/K_v \approx 7$. From Table 4, this value can be achieved using the motor in the KAZ with $G = 5.2$ which indicates that using an EDWS based on an existing motor system could drastically decrease the ground-run distance of small airplanes.

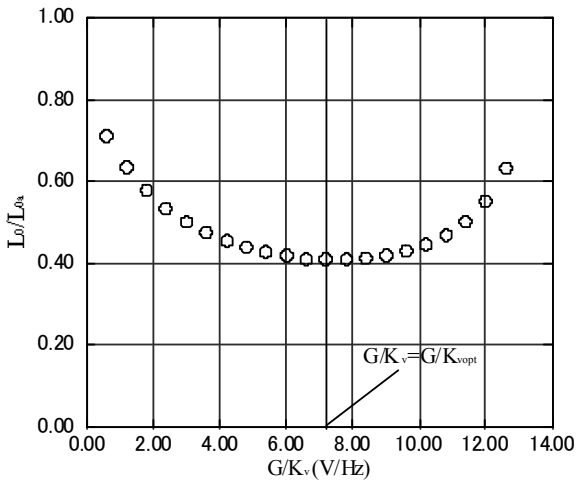


Fig. 7 Analytical result of the relation between L_0/L_{0a} and G/K_v for a Cessna Skyhawk 172 equipped with the motor systems of KAZ.

6 Effects on Flight Performance

Although an EDWS has the potential to decrease ground-run distance, the weight of an EDWS estimated as the sum of the weights of the motor W_m , the controller W_c and battery W_b , is not usually light for small airplanes. In fact, the total of W_m and W_c for the KAZ is about 490N from Table 4. Using a recently developed lithium-ion battery with a high power-weight ratio (3.5kW/kg)[15], W_b is about 590N. Therefore, the total weight of an EDWS is about 1080N. To equip an airplane with an EDWS, the fuel on board has to be cut to maintain the maximum takeoff weight. For a Cessna Skyhawk 172 with a fuel tank volume of 0.2m^3 , the total weight of fuel is calculated to be 1471.5N from specific weight of gasoline 0.71. Subtracting the weight of the EDWS from the fuel weight calculated above, the available fuel weight decreases to 391.5N. The range R_a also decreases from a normal range of $R_{a0} = 1270\text{km}$

to 338km, assuming R_a is proportional to fuel weight.

Figure 8 shows the relationship between L_0/L_{0a} and R_a/R_{a0} for various values of E and G/K_v or for different capacities of the supplied reciprocating engine. L_0/L_{0a} and R_a/R_{a0} become smaller for higher E . This is due to the increase of W_b needed to obtain larger torque at high velocity. Furthermore, L_0/L_{0a} and R_a/R_{a0} are in trade-off relation with respect to the optimum design point ($G/K_v = G/K_{vopt}$ in Fig. 7) for each value of E . On the other hand, installing a larger reciprocating engine (increasing propeller thrust) can also decrease L_0/L_{0a} . However, the effect of the weight increase on the decrease of R_a/R_{a0} is much greater than that of an EDWS. Fitting an EDWS can provide a larger R_a/R_{a0} at $L_0/L_{0a} < 0.75$ than increasing the capacity of the reciprocating engine, indicating the advantage of an EDWS.

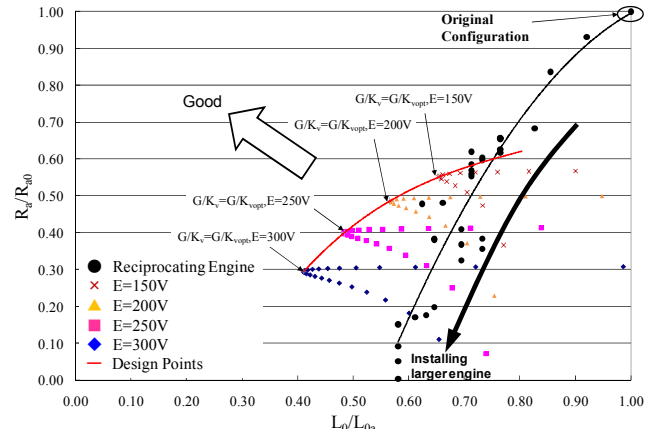


Fig. 8 Analytical results of the trade-off relation between R_a/R_{a0} and L_0/L_{0a} for a Cessna Skyhawk 172 equipped with the motor systems of KAZ or larger reciprocating engines.

7 Summary

A new ground-run method using electrically driven wheels for the landing gear was proposed. The results of experimental and analytical investigation led to the following conclusions.

- 1) Concurrent operation of an EDWS and propeller can drastically decrease ground-run distance compared to the conventional takeoff method.
- 2) Fitting an EDWS improves propulsion efficiency during the ground-run.
- 3) Ground-run distance and range are in a trade-off relation and there is an optimum

- design point in the case of an EDWS using a standard EV motor system.
- 4) Using an EDWS to decrease ground-run distance has the advantage over just increasing engine capacity of requiring a smaller sacrifice of range.

References

- [1] NASA Langley Research Center (1976) "Powered-Lift Aerodynamics and Acoustics." *NASA-SP-406*.
- [2] NAL Flight Test Team, STOL Research Aircraft Project Group 1 (1991) "Evaluation of High Lift Devices of the Quiet STOL Experimental Aircraft ASKA" *NAL-TR-1102*(in Japanese)
- [3] NAL Flight Test Team, STOL Research Aircraft Project Group 1 (1991) "Aerodynamic Characteristics Obtained from α Sweep Test of the Quiet STOL Experimental Aircraft ASKA" *NAL-TR-1112*(in Japanese)
- [4] Hiroshi Shimizu (2002) "The Multi Purpose Electric Vehicle; KAZ" *FED Review* vol.2 no.8(in Japanese)
- [5] Vanausdal, R. K. (1983) "Design, manufacture and test of a prototype powered wheel for aircraft." NASA-CR-172242
- [6] The Boeing Company News Releases (Aug.1, 2005) http://www.boeing.com/news/releases/2005/q3/nr_050801a.html
- [7] The Boeing Company. "Aircraft Wheel Drive Apparatus and Method." *United States Patent* 3977631. (Aug.31, 1976)
- [8] GREENLITE, LTD. "Aircraft Landing-gear Driving System." *PCT Patent* WO9529094. (Nov.02, 1995)
- [9] Hiroshi Kobayashi and Akira Nishizawa (2008) "Study on an Electric Drive System for Ground-roll of Small Airplanes" *JAXA-RR-07-028*(in Japanese)
- [10] H. B. Pecejka and E. Bakker. (1991) "The Magic Formula tyre model." *In Proc. 1st International Colloquium on Tyre Models for Vehicle Dynamics Analysis*, Delft, Netherlands.
- [11] Yoshimasa Tsuruoka, Yasushi Toyoda and Yoichi Hori (1998) "Basic Study on Traction Control of Electric Vehicle" *The transactions of the Institute of Electrical Engineers of Japan. D*, A publication of Industry Applications Society 118-D, 1, pp.45-50. (in Japanese)
- [12] <http://cessna.com/>
- [13] <http://www.allstar.fiu.edu/AERO/BA-Background.htm>
- [14] <http://www.goodyearaviation.com/tiredatabook.html>
- [15] [http://techon.nikkeibp.co.jp/article/EVENT_LEAF/20051021/109931/\(in Japanese\)](http://techon.nikkeibp.co.jp/article/EVENT_LEAF/20051021/109931/(in Japanese))

Copyright Statement

The authors confirm that they, and/or their company or organization, hold copyright on all of the original material included in this paper. The authors also confirm that they have obtained permission, from the copyright holder of any third party material included in this paper, to publish it as part of their paper. The authors confirm that they give permission, or have obtained permission from the copyright holder of this paper, for the publication and distribution of this paper as part of the ICAS2010 proceedings or as individual off-prints from the proceedings.